

Structural Features That Stabilize Halophilic Malate Dehydrogenase from an Archaeobacterium

O. Dym, M. Mevarech, J. L. Sussman*

The high-resolution structure of halophilic malate dehydrogenase (hMDH) from the archaeobacterium *Haloarcula marismortui* was determined by x-ray crystallography. Comparison of the three-dimensional structures of hMDH and its nonhalophilic congeners reveals structural features that may promote the stability of hMDH at high salt concentrations. These features include an excess of acidic over basic residues distributed on the enzyme surface and more salt bridges present in hMDH compared with its nonhalophilic counterparts. Other features that contribute to the stabilization of thermophilic lactate dehydrogenase and thermophilic MDH—the incorporation of alanine into α helices and the introduction of negatively charged amino acids near their amino termini, both of which stabilize the α helix as a result of interaction with the positive part of the α -helix dipole—also were observed in hMDH.

Organisms that grow in hypersaline environments, such as the Dead Sea and the Great Salt Lake, have developed various mechanisms to overcome the extracellular osmotic pressure. Whereas halophilic eubacteria and eukaryotes synthesize large quantities of small organic osmoprotectants (1), halophilic archaeobacteria accumulate inorganic ions within the cell at concentrations exceeding that of the environment. Consequently, the entire biochemical machinery of halophilic archaeobacteria must be adapted to function at high salt concentrations (2). Halophilic enzymes, although they catalyze reactions identical to those mediated by their nonhalophilic congeners, actually require high salt concentrations, in the range of 1 to 4 M, both for stability and for enzymatic activity. These enzymes also possess an excess of acidic over basic amino acid residues (3).

We have now solved the x-ray crystal structure, at 3.2 Å resolution, of the halophilic enzyme hMDH from *Haloarcula marismortui*. This enzyme has been studied extensively (4) by a wide range of biochemical and biophysical methods. On the basis of these earlier studies, a model was proposed in which the stabilization mechanisms of hMDH vary with the solvent environment. In NaCl and KCl solutions, stability would be dominated by the formation of a hydrated salt ion network coordinated by the acidic groups on the protein surface. Nonhalophilic proteins that lack this protective shell tend to aggregate at high salt concentrations (4, 5). The hMDH gene has been cloned and sequenced and expressed in *Escherichia coli* (6). The tetrameric en-

zyme has a predicted molecular mass of 130,552 daltons and contains 303 amino acids per monomer. Its amino acid composition shows a characteristic excess of acidic residues (Asp and Glu constitute 20.5% of all residues) over basic residues (Lys and Arg constitute 7.6% of all residues), and hMDH is stable only at high salt concentrations. The homotetrameric structure of the enzyme has been well established from solution studies (4, 7). At low salt concentrations (<2 M NaCl), dissociation of the tetramer occurs, accompanied by inactivation and denaturation of the protein (4, 8). However, the coenzyme, the reduced form of nicotinamide adenine dinucleotide (NADH), protects hMDH from inactivation at low salt concentrations (9). Sequence alignment (6) shows that hMDH is similar to both lactate dehydrogenase (LDH) and nonhalophilic MDH; the sequence identity with LDHs is ~37% and with MDHs ~20%. Furthermore, the replacement of Gln¹⁰⁰ of *Bacillus stearothermophilus* LDH by Arg resulted in a change in specificity to that characteristic of MDH (10), whereas replacing Arg¹⁰⁰ in hMDH by Gln (6) changed the substrate specificity from oxaloacetate to pyruvate, thus reinforcing the structural resemblance of hMDH to LDH.

Crystals of hMDH were grown at 19°C (11) with methylpentanediol (MPD) as a precipitant. Two data sets were collected, one at room temperature and the other at -10°C (Table 1). The structure of the binary complex hMDH-NADH was determined to 3.2 Å resolution by the molecular replacement method, with the dogfish LDH (dLDH) structure as a model (12). The phases were substantially improved by electron-density averaging followed by solvent flattening. The primary, secondary, and tertiary structures of hMDH are similar to those of dLDH, which consists of a tetramer of four identical subunits with one

Table 1. Data collection statistics for hMDH. Crystals were grown for both the C (C222₁; parameters: $a = 114.57$, $b = 130.57$, $c = 123.77$ Å) and P (P2₁2₁2₁; parameters: $a = 115.00$, $b = 128.05$, $c = 123.53$ Å) forms by vapor diffusion according to the hanging drop technique at 19°C, with MPD as the precipitant. The 7- μ l drops contained hMDH (10 mg/ml) in a solution containing 1.8 M NaCl, 1 mM NADH, 50 mM sodium phosphate (pH 7), and 58% MPD. The 1-ml reservoir contained 60 to 70% MPD. Under these conditions (absence of salt in the reservoir), water evaporates from the reservoir into the drop, thereby increasing the drop volume up to four times and resulting in a final concentration of ~0.5 to 0.8 M NaCl. The presence of NADH in the crystallization solution prevents inactivation of the enzyme (9). X-ray data for two crystal forms were collected with a Siemens/Xentronics area detector mounted on a Rigaku rotating anode x-ray generator and were processed with the XDS data reduction program (21). The structures were solved in both crystal forms by the molecular replacement technique with the programs MERLOT (22) and AMORE (23), with dLDH (12) as a model. Phases were improved by means of electron-density averaging followed by solvent flattening, with the use of the DEMON (24) package. Two approaches of phase improvement were applied in solving the crystal structure of hMDH: averaging four copies in the P form and averaging six copies between the two different crystal forms (P and C). On the basis of these averaged maps, major portions of the chain could be traced, and differences in the amino acid sequences between dLDH and hMDH could be easily identified, with the use of the program O (25). There was no apparent bias from the initial phased model that had been derived from the dLDH structure as seen in clear electron density corresponding to the coenzyme NADH, although the NADH was not included in the calculations. Manual model building was performed on both the C and combined P and C averaged maps, because some portions were better resolved either in one map or in the other. Refinements were performed on the C crystal form with the use of X-PLOR (26), resulting in an R factor of 18.2% and free- R of 28.0% for all data at 10 to 3.2 Å resolution. The root mean square deviations in the refined hMDH structure are 0.014 Å for bond lengths and 2.01° for bond angles. Coordinates are available from the Brookhaven Protein Data Bank (27) (IDCODE: 1HLP). Refinement of the P crystal form is in progress.

Statistic	Crystal form	
	C	P
Subunits in the asymmetrical unit	2	4
Maximum resolution (Å)	3.24	2.9
Temperature (°C)	RT*	-10
Data collection duration (hours)	16	48
Time per frame (s)	240	120
Unique measured reflections (no.)	12,508	37,235
Unique possible reflections (no.)	14,158	41,104
Completeness of data (%)	88.3	90.5
$\dagger R_{sym}$ (%)	8.7	8.4

*RT, room temperature. $\dagger R_{sym} = \frac{\sum (I - I_{avg})}{\sum I_{avg}}$, where I is diffraction intensity and I_{avg} is mean intensity.

O. Dym and J. L. Sussman, Department of Structural Biology, Weizmann Institute of Science, Rehovot 76100, Israel.

M. Mevarech, Department of Molecular Microbiology and Biotechnology, Tel Aviv University, Ramat Aviv 69978, Israel.

*To whom correspondence should be addressed.

NADH binding site per subunit (12). The major difference between the two enzymes is the large excess of acidic over basic residues in hMDH (Fig. 1A), which contrasts with the approximately equal numbers of acidic and basic residues in dLDH (Fig. 1B). The acidic residues in hMDH appear mostly on the surface of the tetramer. This observation was verified by accessible-surface area calculations of acidic versus basic residues performed with the algorithm of Lee and Richards (13). These calculations showed that the hMDH surface possesses twice as many acidic as basic residues, whereas dLDH displays approximately equal numbers. Some of the additional acidic residues in hMDH are located across the interdimer surface, which causes the two dimers (comprising monomers 1 and 3 and 2 and 4) (Fig. 1A) to repel each other, so that the hMDH tetramer is wider than that of dLDH by ~ 10 Å. In dLDH, contacts at this interface consist primarily of hydrophobic interactions between amino acid side chains and are dominated by the interactions with the NH_2 -terminal "arm" (the first 20 amino acids, which are missing in hMDH). Some of these interactions are absent from hMDH also because of the tetramer widening and substitutions by

acidic residues. The hMDH interface contacts consist solely of two salt-bridge clusters situated at the two extremities of the interdimer surface (Fig. 2).

The tetramer surface of hMDH is coated with acidic residues, whereas MDHs and LDHs from other sources lack this feature. The net charge of the hMDH tetramer is -156 , compared with $+16$ for the dLDH tetramer. Whereas dLDH displays both positive and negative isopotential surfaces, the hMDH tetramer is characterized by an unusually large negative isopotential surface that covers it entirely (Fig. 3, A and B). Calculation of the potential surfaces of both hMDH and dLDH at a salt concentration of 0.7 M does not have a marked effect for dLDH but has a large effect on hMDH (Fig. 3C), resulting in a more balanced overall distribution of positive and negative potentials. Similar isopotential surfaces are observed whether 0.7 or 4 M salt is assumed, indicating that 0.7 M salt is sufficient to screen the excess acidic residues in hMDH.

The large excess of acidic residues on the surface of hMDH may play several roles. The fact that, at physiological pH, acidic residues, especially Glu, are capable of binding more water than other residues (14)

may contribute to the creation of a hydration sphere that protects the enzyme from aggregating at high salt concentrations. Nonhalophilic proteins, which lack such a protective shell, tend to aggregate at salt concentrations of >1 M. Another function of the acidic residues in hMDH is the stabilization of the folded native protein conformation by participation in an unusually large number of salt bridges. Interactions between nitrogen atoms of basic residues (Arg and Lys) and oxygen atoms of acidic residues (Glu and Asp) are widely observed in proteins. The ionic nature of these hydrogen bonds results in an interaction energy that is greater by an order of magnitude than that between neutral moieties (15). The hMDH subunit contains 15 Arg residues, three of which (Arg¹⁰⁰, Arg¹⁶⁹, and Arg¹⁷¹) are in conserved regions that constitute the active site. All the remaining Arg side chains are in close contact with at least one oxygen of an acidic residue, creating salt-bridge clusters. In the contact region between the two dimers, two salt-bridge clusters (Fig. 2) are located at the opposite extremes of the interface.

Comparison of the structures of the thermophilic proteins *B. stearothermophilus* LDH (16) and *Thermus flavus* MDH (17) with those of mesophilic LDHs and MDHs, respectively, has revealed unique structural features of the thermophilic enzymes that may contribute to their thermostability. Many of these structural features are also present in hMDH; in particular, the large number of salt bridges. Indeed, salt bridges are both more abundant and stronger in hMDH than in the mesophilic as well as in

Fig. 1. Comparison of the three-dimensional tetramer structures of hMDH (A) and dLDH (B). Red balls, acidic residues; blue balls, basic residues. The numbers 1 to 4 indicate four different monomers. The accessible surface area of hMDH was calculated with the algorithm of Lee and Richards (13): Monomers 1 and 3 account for loss of 33.6% of the surface on dimerization [$(2 \times \text{monomer}) - \text{dimer}$], monomers 1 and 2 account for loss of 13%, and monomers 1 and 4 account for no reduction in surface area. The surface area reductions on dimerization for dLDH are 32.2, 19.3, and 9.9%, respectively.

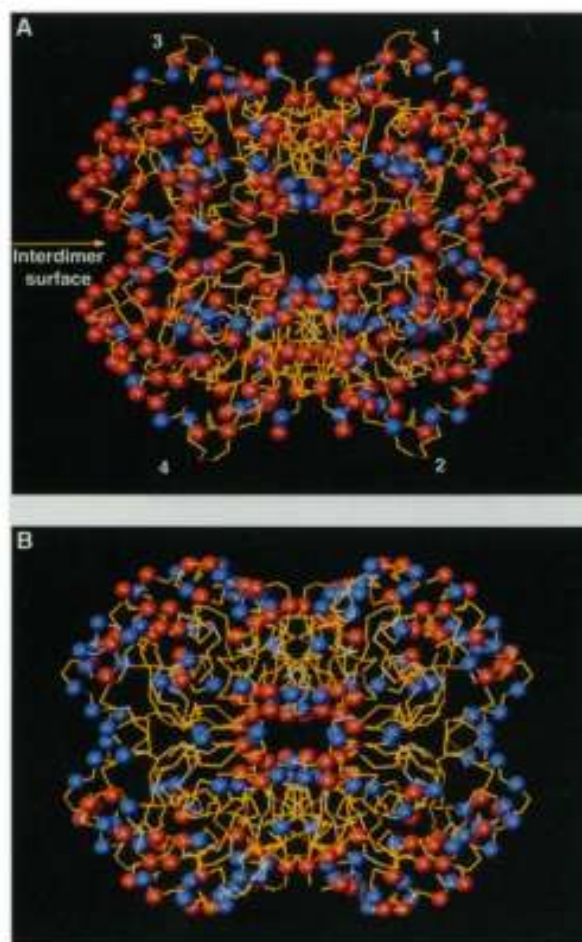


Fig. 2. One of the two salt-bridge clusters found along the dimer-dimer interface of hMDH (between monomers 1 and 3, and monomers 2 and 4). This cluster involves interactions between Arg²⁰⁵ (R205) from two subunits, denoted as a and b, and Glu (E186) and Asp (D210) residues from each subunit. Some of these interactions are inter- as well as intramolecular and use twin N-twin O; for example, the interaction between E186a and R205b and the corresponding symmetrical interaction between E186b and R205a.

the thermophilic enzymes (Table 2). The existence of clusters in which Arg residues are in close contact with more than one acidic residue is unique to hMDH in comparison with other LDHs and MDHs. Moreover, in hMDH, many of these clusters involve interactions between secondary structural elements, further stabilizing the three-dimensional structure. Although it may appear surprising that salt bridges are stable at high salt concentrations, surface salt bridges have been shown to contribute to protein stability at a salt concentration of 0.5 M (18); it is thus conceivable that their contribution to stability may be significant at even higher salt concentrations. Given that, in the presence of NADH, hMDH is stable even at low salt concentrations (9), it is likely that the crystal structure of the enzyme at 0.8 M salt is similar to that at higher salt

concentrations. The explicit visualization of the salt ions in stabilizing the folded conformation awaits the determination of the hMDH structure at higher resolution.

Two structural features observed in α helices of thermophilic proteins are known to enhance thermostability: an increased number of Ala residues and the location of acidic residues at the NH₂-terminus (19, 20). The enzyme hMDH, like *T. flavus* MDH, has more alanines in its α helices than are present in those of mesophilic or nonhalophilic MDHs or LDHs. Consequently, intrahelical hydrophobic interactions are strengthened and the helices are stabilized. Introduction of negatively charged amino acids at the NH₂-terminus of an α helix increases the thermostability of phage T₄ lysozyme as a result of an electrostatic interaction with the helix dipole (19, 20). A search for helix stabilization in hMDH, as

compared with other LDHs and MDHs, revealed the following substitutions: Lys⁵⁷→Asp, Lys²²⁵→Glu, Ser²⁴⁰→Glu, Lys³⁰⁶→Asp, and Pro³⁰⁷→Asp. These acidic residues are all located at the NH₂-termini of α helices in hMDH, thus increasing their stability.

Both thermophiles and halophiles live in extreme environments and share many unusual properties. However, on the basis of the x-ray structure of hMDH, the extreme halophiles appear to show these properties to a much greater extent than the thermophiles.

REFERENCES AND NOTES

1. L. J. Borowitzka and A. D. Brown, *Arch. Microbiol.* **96**, 37 (1974); L. Gustafsson and B. Norkrans, *ibid.* **110**, 177 (1979); P. H. Yancey, M. E. Clark, S. C. Hand, R. D. Bowler, G. N. Somero, *Science* **217**, 1214 (1982).
2. H. Eisenberg, M. Meverach, G. Zaccari, *Adv. Protein Chem.* **43**, 1 (1992).
3. J. K. Lanyi, *Bacteriol. Rev.* **38**, 272 (1974).
4. F. Bonneté, C. Ebel, G. Zaccari, H. Eisenberg, *J. Chem. Soc. Faraday Trans.* **89**, 2659 (1993).
5. F. Bonneté, D. Madem, G. Zaccari, *J. Mol. Biol.* **244**, 436 (1994).
6. F. Cendrin, J. Chroboczek, G. Zaccari, H. Eisenberg, M. Meverach, *Biochemistry* **32**, 4308 (1993).
7. E. Daniel, A. Azem, I. Shaked, M. Meverach, *Comp. Biochem. Physiol.* **106B**, 401 (1993).
8. M. Meverach, H. Eisenberg, E. Neumann, *Biochemistry* **16**, 3781 (1977).
9. K. Hecht and R. Jaenicke, *ibid.* **28**, 4979 (1989).
10. A. R. Clarke, T. Atkinson, J. J. Holbrook, *Trends Biochem. Sci.* **14**, 145 (1989).
11. A. Moftherson, *Methods Enzymol.* **114**, 120 (1985).
12. C. Abad-Zapatero, J. P. Griffith, J. L. Sussman, M. G. Rossmann, *J. Mol. Biol.* **198**, 445 (1987).
13. B. K. Lee and F. M. Richards, *ibid.* **55**, 379 (1971).
14. I. D. Kuntz and W. Kauzmann, *Adv. Protein Chem.* **28**, 239 (1974).
15. J. Singh, J. M. Thornton, M. Snarey, S. F. Campbell, *FEBS Lett.* **224**, 161 (1988).
16. K. Piontek, P. Chakrabarti, H. P. Schär, M. G. Rossmann, H. Zuber, *Protein Struct. Funct. Genet.* **7**, 74 (1990); H. Zuber, *Bioophys. Chem.* **29**, 171 (1988); F. Zöll, R. Schneller, R. Ufer, H. Zuber, *Biol. Chem. Hoppe Seyler* **372**, 363 (1991).
17. C. A. Kelly, M. Nishiyama, Y. Ohnishi, T. Beppu, J. J. Birkhoff, *Biochemistry* **32**, 3913 (1993).
18. A. Horovitz, L. Serrano, B. Avron, M. Bycroft, A. R. Fersht, *J. Mol. Biol.* **216**, 1031 (1990).
19. A. Nicholls, K. A. Sharp, B. Honig, *Protein Struct. Funct. Genet.* **11**, 281 (1991).
20. H. Nicholson, D. E. Anderson, S. Dao-pin, B. W. Matthews, *Biochemistry* **30**, 9816 (1991).
21. W. Kabsch, *J. Appl. Crystallogr.* **21**, 67 (1988).
22. P. M. Fitzgerald, *ibid.*, p. 273.
23. J. Navaza, *Acta Crystallogr.* **A50**, 157 (1994).
24. F. M. D. Velleux, thesis, University of Groningen, Netherlands (1990).
25. T. A. Jones, J. Y. Zou, S. W. Cowan, M. Kjeldgaard, *Acta Crystallogr.* **A47**, 110 (1991).
26. A. T. Brünger, *X-PLOR A System for X-ray Crystallography and NMR*, 3.1 Manual (Yale Univ. Press, New Haven and London, 1992).
27. F. C. Bernstein et al., *J. Mol. Biol.* **112**, 535 (1977).
28. This paper is dedicated to Henryk Eisenberg for inspiring us to begin this research. We thank I. Silman, M. Harel, F. Frolow, G. Cohen, G. Zaccari, and C. Felder for their discussions and comments on the manuscript, and E. Pras, R. Ravelli, and M. Raves for help in preparation of the figures. Supported by the Kimmelman Center for Biomolecular Structure and Assembly, Rehovot, and the Association Franco-Israélienne pour la Recherche Scientifique et Technologique.

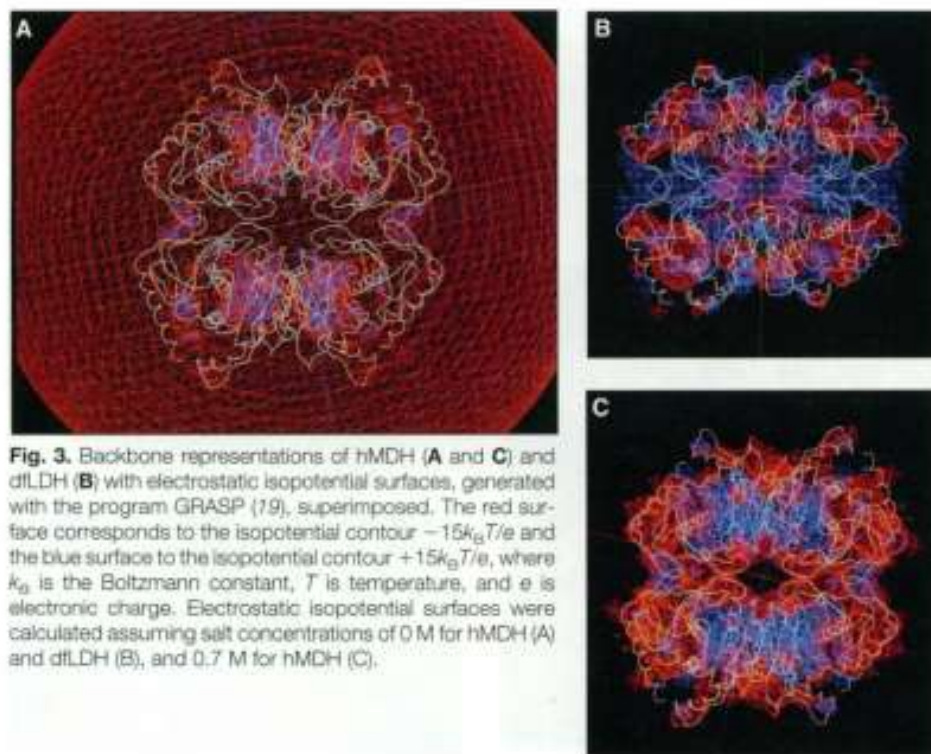


Fig. 3. Backbone representations of hMDH (A and C) and dLDH (B) with electrostatic isopotential surfaces, generated with the program GRASP (19), superimposed. The red surface corresponds to the isopotential contour $-15k_B T/e$ and the blue surface to the isopotential contour $+15k_B T/e$, where k_B is the Boltzmann constant, T is temperature, and e is electronic charge. Electrostatic isopotential surfaces were calculated assuming salt concentrations of 0 M for hMDH (A) and dLDH (B), and 0.7 M for hMDH (C).

Table 2. Salt bridges containing Arg present in nonhalophilic LDH, cytoplasmic MDH, and hMDH enzymes. Dashes indicate the number of salt bridges is 0. *B. stear.*, *Bacillus stearothermophilus*.

Enzyme	Total Arg per monomer subunit	Salt bridges (no.)					
		Intra-molecular	Inter-molecular	Arg-Asp/Glu	Arg-2(Asp/Glu)	2(Arg)-4(Asp/Glu)	2(Arg)-5(Asp/Glu)
Dogfish LDH	8	2	—	2	—	—	—
<i>B. stear.</i> LDH	15	5	—	5	—	—	—
Mouse LDH	10	1	—	1	—	—	—
Porcine heart LDH	8	1	—	1	—	—	—
Porcine muscle LDH	11	3	—	3	—	—	—
Cytoplasmic MDH	10	5	1	2	2	—	—
Halophilic MDH	15	14	8	3	5	1	1